Doped t-J model on a triangular lattice: Possible application to $Na_xCoO_2 \cdot yH_2O$ and $Na_{1-x}TiO_2$

Qiang-Hua Wang,[1] Dung-Hai Lee,[2] and Patrick A. Lee[3]
[1]*National Laboratory of Solid State Microstructures, Institute for Solid State Physics, Nanjing University, Nanjing 210093, China*
[2]*Department of Physics, University of California at Berkeley, Berkeley, California 94720, USA*
[3]*Department of Physics, Massachusetts Institute of Technology, Cambridge, Massachusetts 02139, USA*
(Received 4 November 2003; published 12 March 2004)

We report the finding of time-reversal-symmetry-breaking $d_{x^2-y^2}+id_{xy}$ superconducting ground state in the slave-boson mean-field theory for the t-J model on triangular lattice. For $t/J=-5(t/J=-9)$ pairing exists for $x<13\%$ ($x<8\%$) upon electron doping, and $x<56\%$ ($x<13\%$) upon hole doping. These results are potentially relevant to doped Mott insulators $Na_xCoO_2 \cdot yH_2O$ and $Na_{1-x}TiO_2$.

DOI: 10.1103/PhysRevB.69.092504 PACS number(s): 74.25.Jb, 71.27.+a, 79.60.Bm

There is now broad agreement that the physics of the high-T_c cuprate is that of the doped Mott insulator. However, 17 years after its discovery[1] the layered cuprates remain the only materials which exhibit the phenomenon of high-T_c superconductivity. There are three reasons which make the cuprates unique: (1) The parent compound is a Mott insulator with $S=\frac{1}{2}$ and no orbital degeneracy; (2) the structure is two dimensional; and (3) the exchange energy J is very large ($J\approx 1500$ K). Anderson[2] has stressed the strong quantum fluctuation of the $S=\frac{1}{2}$ system in two dimensions. His resonating valence bond (RVB) theory describes a liquid of spin singlet which becomes a superconductor when the holes are phase coherent. If this is a general property of a doped Mott insulator, it will clearly be desirable to examine other examples which satisfy these three criteria. Recently Takada *et al.*[3] reported the discovery of superconductivity in $Na_xCoO_2 \cdot yH_2O$ with a T_c of 5 K for $x=0.35$. As these authors pointed out, this system may be viewed as a Mott insulator with electron doping of 35%. The Co atoms are in a triangular lattice and the Co^{4+} atom is in a low spin ($S=\frac{1}{2}$) state. Thus this material satisfies the first two criteria listed above. The value of J is not known at present, but the new discovery offers hope that a second system which exhibits superconductivity by doping a Mott insulator may be realized. A summary of what is known about this material and a discussion in terms of RVB physics was given by Baskaran.[4] In this paper we argue that the t-J model on a triangular lattice is a reasonable starting point to model these materials. We estimate the value of J, and compute the slave-boson mean-field phase diagram for both electron and hole doping. We find $d_{x^2-y^2}+id_{xy}$ pairing over significant range of doping for both $t/J=-5$ and $t/J=-9$. The appearance of superconductivity shows an interesting particle-hole asymmetry. We propose that $Na_{1-x}TiO_2$ may be an example of the hole-doped system.

The transition-metal oxide layers in Na_xCoO_2 and $Na_{1-x}TiO_2$ form a common structure where the transition metal is surrounded by an octahedral oxygen cage. The cages are edge sharing, forming a layered structure. The stacking of the oxide layers is different in the two materials and we first describe the structure of $Na_{1-x}TiO_2$. A way to visualize the structure which is convenient for understanding the electronic structure is shown in Fig. 1(a). It shows a piece of the crystal structure in a coordinate system which is standard for the oxygen octahedron. The hexagonal layered structure is visualized by looking down on this structure along the (1,1,1) direction. Thus the axis z' becomes the c axis in the layered hexagonal structure notation. One can see stacking of O-Ti-O or O-Co-O hexagonal layers, highlighted in Fig. 1(b), separated by a Na layer. In $Na_{1-x}TiO_2$, the Na sits directly over the oxygen in the layer below Ti (vertices of the dashed triangle), whereas in Na_xCoO_2, the Na site is on top of the Co. The next CoO_2 layer has Co on top of Na but the stacking order of the oxygen layer is reversed (solid triangle now lies below Co) thereby doubling the unit cell along c. This difference in stacking does not affect the electronic structure of the CoO_2

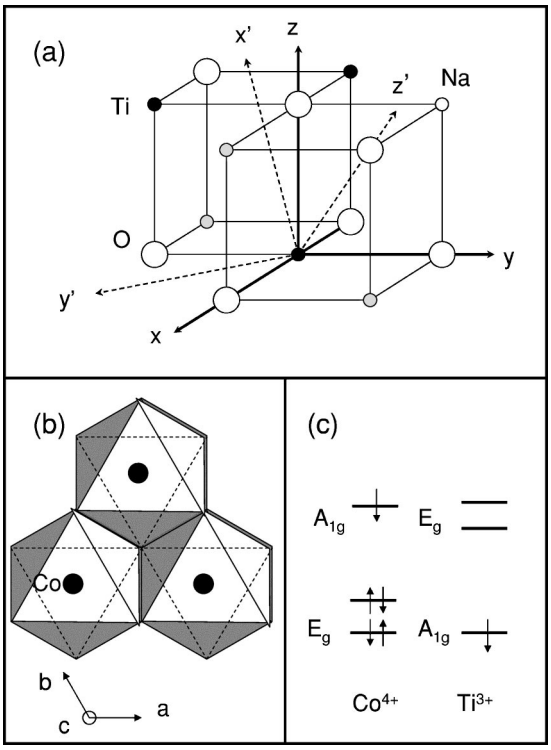

FIG. 1. (a) The $NaTiO_2$ structure. (b) Projection of (a) along the (1,1,1) direction showing the oxide layer. This layer is similar in Na_xCoO_2 and $NaTiO_2$. Oxygen occupies vertices of the solid (dashed) triangles which lie above (below) the cobalt or titanium layers. (c) The splitting of the t_2g levels due to the distortion of the oxygen octahedra as given in (a) (adopted from Ref. 5).

layers and will be ignored from now on.

From Fig. 1(a) it is clear that the d states are split into t_{2g} and e_g orbitals by the octahedral environment. A shift of the oxygen along the (1,1,1) direction splits the t_{2g} orbitals into[5]

$$A_{1g}=(d_{xy}+d_{yz}+d_{zx})/\sqrt{3} \tag{1}$$

and a doublet (labeled E_g to distinguish from e_g)

$$E_g=((d_{zx}-d_{yz})/\sqrt{2},(-2d_{xy}+d_{yz}+d_{zx})/\sqrt{6}). \tag{2}$$

The band calculation of Singh[6] showed that the splitting is fairly large in $Na_{0.5}CoO_2$ with A_{1g} lying higher than E_g. As shown in Fig. 1(c), in Co^{4+} the unpaired spin occupies the nondegenerate A_{1g} orbital. We note that the t_{2g} orbitals have lobes which point to the midpoint of lines connecting the oxygens in the octahedral cage. From Fig. 1(a) and Eq. (1) we see that the A_{1g} orbitals on nearest-neighbor Co have components which point directly at each other. Thus unlike the cuprate, where the hopping is via the Cu-O covalent band, in the cobalt compounds, the direct overlap between the A_{1g} orbitals forms a band. Due to band overlap, it is difficult to extract the A_{1g} bandwidth from Singh's calculations[6] but we estimate it to be between 1 and 1.4 eV. From this we extract the hopping integral t for the t-J model

$$H=-t\sum_{\langle ij\rangle}(Pc^{\dagger}_{i\sigma}c_{j\sigma}P+\text{H.c.})+J\sum_{\langle ij\rangle}\left(\mathbf{S}_i\cdot\mathbf{S}_j-\frac{1}{4}n_in_j\right) \tag{3}$$

to be $t=-0.11--0.15$ eV. In Eq. (3) the projection operator P removes double/zero occupancy for hole/electron doping, respectively. We note that the overlap between A_{1g} orbitals is positive and the negative sign of t is a consequence of the sign convention chosen in Eq. (3). As emphasized by Baskaran,[4] there is no particle-hole symmetry in the triangular lattice and the sign of t is important. Singh's band structure[6] shows a maximum in the band structure at Γ, confirming the negative sign of t. The Fermi surface of $Na_{0.5}CoO_2$ consists of a hole pocket of area $\frac{1}{4}$ around the Γ point.[6] This is consistent with photoemission results.[7]

It is much more difficult to estimate the exchange constant $J=4t^2/U$ because the U parameter is highly uncertain due to screening. We appeal to another $t_{2g}S=\frac{1}{2}$ system where J has been determined experimentally. In TiOCl the t_{2g} orbital is orbitally ordered and forms one-dimensional $S=\frac{1}{2}$ spin chains.[8] The exchange interaction was found to be 660 K by fitting the spin susceptibility to the Bonner-Fisher curve. In this case the t_{2g} orbitals are pure d_{yz} and point directly at each other. The bandwidth from band-structure calculations is also about 1 eV, leading to $t\approx-1/4$ eV. Note that t for Na_xCoO_2 is considerably smaller even though the Co-Co distance at 2.84 Å is shorter than the Ti-Ti distance (3.38 Å). This is because only one component out of three in Eq. (1) points directly towards each other. Assuming that U is similar, our best guess for J is 12–24 meV and $|t/J|\approx 6$–9. Note that our estimate of J for Na_xCoO_2 is about an order of magnitude smaller than that for the cuprates.

It is interesting to consider another $S=\frac{1}{2}$ system which corresponds to single occupation of the t_{2g} orbitals. $NaTiO_2$ has similar layer structure as Na_xCoO_2 but the Na layer is nominally fully occupied. The Ti^{3+} has d^1 configuration giving rise to unpaired $S=\frac{1}{2}$. Contrary to $Na_{0.5}CoO_2$, the A_{1g},E_g splitting is much smaller than the bandwidth, according to local-density approximation (LDA) calculations.[5] However, an LDA+U calculation shows that the A_{1g} orbital is occupied preferentially, so that the single electron again occupies the nondegenerate A_{1g} band.[5] Reduction of the Na occupation ($Na_{1-x}TiO_2$) corresponds to doping by x holes. The undoped system is of great interest because it is one of the few known examples of the $S=\frac{1}{2}$ triangular antiferromagnet. However, the control of Na stoichiometry presents a serious materials challenge and relatively few studies have been carried out to date.[9]

As we mentioned earlier the occupation constraint of Eq. (3) is different for the electron and hole doping. In the case of electron doping we shall perform a particle-hole transformation $c_{i,\sigma}\rightarrow c^{\dagger}_{i,-\sigma}$ so that the constraint always means no double occupancy and the sign of t is reversed. Consequently $t<0$ for hole-doped $Na_{1-x}TiO_2$ and $t>0$ for electron-doped Na_xCoO_2.

The starting point of our calculation is the following U(1) slave-boson mean-field Hamiltonian[10] for the t-J model at hand, $H_{MF}=H_{nm}+H_m$ with

$$H_{nm}=-\sum_{\langle ij\rangle\sigma}\left[\left(t\sqrt{x_ix_j}+\frac{3J}{8}\chi^{*}_{ij}\right)f^{\dagger}_{i\sigma}f_{j\sigma}+\text{H.c.}\right]$$
$$-\frac{3J}{8}\sum_{\langle ij\rangle\sigma\sigma'}[\Delta^{*}_{ij}f_{i\sigma}f_{j\sigma'}\epsilon_{\sigma\sigma'}+\text{H.c.}]-\sum_{i\sigma}\mu_in_{i\sigma};$$

$$H_m=J\sum_{\langle ij\rangle}(\mathbf{S}_i\cdot\mathbf{m}_j+\mathbf{S}_j\cdot\mathbf{m}_i). \tag{4}$$

Here $x_i=1-\Sigma_\sigma\langle n_{i\sigma}\rangle$ and μ_i is the corresponding local Lagrange multiplier. The doping level is given by $x=\Sigma_i x_i/N$ with N the lattice sites. The mean-field order parameters are $\chi_{ij}=\Sigma_\sigma\langle f^{+}_{i\sigma}f_{j\sigma}\rangle$, $\Delta_{ij}=\Sigma_{\sigma\sigma'}\epsilon_{\sigma\sigma'}\langle f_{i\sigma}f_{j\sigma'}\rangle$, and $\mathbf{m}_i=\langle\mathbf{S}_i\rangle$ with $\mathbf{S}_i=\Sigma_{ss'}\boldsymbol{\sigma}_{ss'}f^{\dagger}_{is}f_{is'}/2$. Note that a general noncollinear magnetic order is allowed.

Our search for the mean-field solution proceeds in two stages. First we assume the density to be uniform and perform an unrestricted search of the parameters χ_{ij}, Δ_{ij}, and $\mathbf{m}_i$ (over 6×6 elementary unit cells in a large lattice). For $x<x_c$ we find χ_{ij} to be a real constant as long as x is nonzero and $\Delta_{ij}=0$ while the spins form the $\sqrt{3}\times\sqrt{3}$ noncollinear structure identified by Huse and Elser[11] for $x=0$. If we denote the lattice by $\mathbf{r}_i=n\mathbf{a}+l\mathbf{b}$, $\mathbf{a}=\hat{x}$, and $\mathbf{b}=-\frac{1}{2}\hat{x}+(\sqrt{3}/2)\hat{y}$, then a representative solution has $m^z_i=0$ and $m^x_i+im^y_i=|\mathbf{m}|e^{i\mathbf{Q}\cdot\mathbf{r}_i}$, where $\mathbf{Q}=(2\pi/3,2\pi/\sqrt{3})$ and $\mathbf{Q}\cdot\mathbf{r}_i=2\pi/3(n+l)$. $|\mathbf{m}|=\frac{1}{2}$ at zero doping, and decreases gradually with increasing doping. It is roughly 0.35–0.38 (depending on our choices of t/J) at $x=x_c$, where the long-range ordered magnetic state undergoes a first-order phase transition into a uniform $d_{x^2-y^2}\pm id_{xy}$ superconducting state. The value of x_c is 3.8%, 3.7%, 2.2%, 2.1% for $t/J=5,-5,9,-9$, respectively. Even if the pairing channel is removed, the magnetic order extends only up to $x_*=4.5\%$, 4.2%,

2.4%, 2.4% for the same set of t/J. This is significantly different from the mean-field solution of the square lattice with $t/J=3$ as appropriate for the cuprates. In that case the system is inhomogeneous with alternating stripes of superconducting and magnetic regions at roughly $2\% \leqslant x \leqslant 12\%$, and the magnetic order becomes commensurate with coexisting uniform pairing order at higher doping levels up to $x_c \sim 20\%$.[12] For the hexagonal lattice, the stable region of the antiferromagnetic solution is greatly reduced. This is reasonable in view of the frustration of the lattice, which disfavors magnetic order and was the original motivation of the RVB as a competing state.[2]

In the second stage of the calculation we concentrate on doping greater than x_c. In view of the first-order nature of the transition to magnetic order, we shall present results without magnetic order even for $x<x_c$, with the understanding that the solution is only locally but not globally stable. We suppress magnetic order and perform an unrestricted search for solutions of H_{nm} in Eq. (4) on a 400×400 lattice. In the elementary unit cell (varied from 1×1 up to 4×8) we put random initial values for χ_{ij}, Δ_{ij}, x_i, and μ_i, and evolve them so that the mean-field free energy is minimized at the desired doping level. Note that this time we allow nonuniform charge density. However, with our choice of parameters, we found spatially nonuniform solutions only for $x<x_u$, where x_u is always less than x_c and these will be ignored from now on. Due to the uncertainty of t/J we have studied two cases $|t/J|=5$ and $|t/J|=9$. It turns out that in both cases there is a significant doping range in which the ground state is superconducting. The pairing symmetry is always $d_{x^2-y^2}+id_{xy}$, hence breaks the time-reversal symmetry. It is interesting to note that if one ignores the magnetic order parameter at zero doping the same mean-field theory predicts a degenerate family of ground states. Among them the $d_{x^2-y^2}+id_{xy}$ paired state and the $\pi/2$ flux state are two examples.[13,14] To visualize the pairing pattern, consider an arbitrary site. The Δ_{ij} associated with the six bonds stemming from it has the form $\Delta_{ij}=\Delta e^{i2\theta_{ij}}$ for $d_{x^2-y^2}+id_{xy}$ pairing and $\Delta_{ij}=\Delta e^{-i2\theta_{ij}}$ for $d_{x^2-y^2}-id_{xy}$ pairing. To generate the pairing field over the entire lattice, simply translate the above pattern to other sites. In the absence of a magnetic field the $d_{x^2-y^2}+id_{xy}$ and $d_{x^2-y^2}-id_{xy}$ pairing are degenerate.

The doping dependence of the zero-temperature pairing order parameter $\Delta=|\Delta_{ij}|$ is plotted in Fig. 2 (solid lines) for $t=5J$ (a), 9 J (b), -5 J (c), and -9 J (d), where we observe that pairing exists for $x\leqslant13\%$ (a), 8% (b), 56% (c), and 13% (d). The peak in Δ at $x=0.5$ in Fig. 2(c) is explained by the Van Hove peak in the free-electron density of states. Also shown in Fig. 2 is the hopping order parameter $\chi=|\chi_{ij}|$ (dashed lines). It is weakly dependent on x for $x<30\%$. Interestingly χ_{ij} has the same sign of t from our calculation. This is a reasonable result as it increases the bandwidth of the fermions so that the kinetic energy is lowered. Finally, a much more important feature in Fig. 2 is the considerable asymmetry between electron doping ($t>0$) and hole doping ($t<0$). This is due to the particle-hole asymmetry in the free-electron dispersion on the triangular lattice. Indeed, the stronger pairing for hole doping is due to the increases in the Fermi-level density of state as the averaged occupation decreases from half filling.

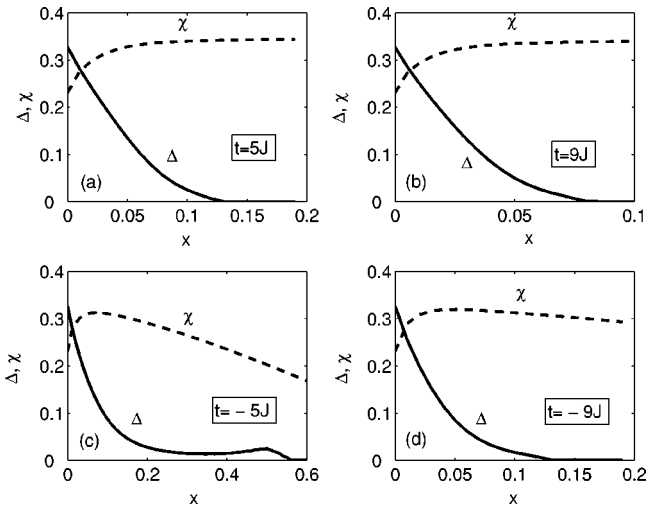

FIG. 2. Dependence of the order parameters on hole doping (x): $t=5$ J (a), 9 J (b), -5 J (c), and -9 J (d). Note the scale change in (b) and (c).

We have also computed the onset temperature of the RVB fermion pairing and Bose-Einstein condensation (BEC) of holons.[15] The mean-field superconducting transition is the smaller of the RVB and BEC curves (Fig. 3). As usual, the Bose condensation temperature is an overestimate of the phase-coherence temperature of the slave bosons. More generally because of the proximity to the Mott insulator limit, we expect that the superconducting transition temperature will be determined by the superfluid density at low doping, and by the onset of pairing at higher doping, forming a phase diagram similar to that of the cuprates. It is worth noting that in the case of cuprates, the thermal excitation of nodal quasiparticles significantly reduces the superfluid density and therefore the transition temperature at low doping.[16,17] The

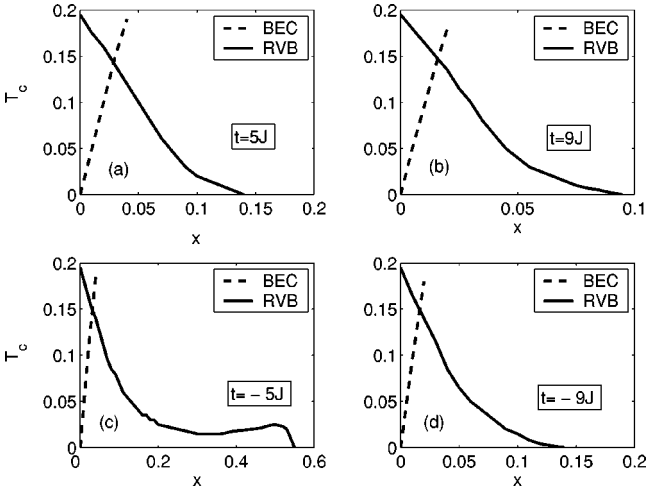

FIG. 3. Dependence of the RVB and BEC critical temperatures (in units of J) on hole doping (x): $t=5$ J (a), 9 J (b), -5 J (c), and -9 J (d). Note the scale change in 2(b) and 2(c).

existence of a full gap in the $d_{x^2-y^2}+id_{xy}$ state suppresses this possibility and everything else being equal, we can expect a higher T_c in this case.

We conclude that within the slave-boson mean-field theory, the systems exhibit noncollinear antiferromagnetism for $x<x_c$. Above this lower critical concentration and below certain upper critical concentration the systems exhibit time-reversal symmetry-breaking $d_{x^2-y^2}+id_{xy}$ pairing state. The orbital moment produces a magnetic field which can be checked by μSR. The field has been estimated to be 15 G for the anyon model[18] but a calculation based on slave boson mean field theory yields a smaller estimate of 1 G near a vacancy.[19] If the orbital moments in neighboring layers are parallel, this state has been predicted to exhibit fascinating effects such as quantized spin Hall conductance and anomalous Hall thermal conductivity.[20] The orbital moment corresponds to roughly $\frac{1}{20}\mu_B$, and field cooling in a modest magnetic field may line up the orbital moments. It will clearly be desirable to achieve such a state in the laboratory. For $|t/J|=5$ ($|t/J|=9$), the $d_{x^2-y^2}+id_{xy}$ superconductor is expected to exist over a low doping range $x<13\%$ ($x<8\%$) for electron doping, and a wider range $x<56\%$ ($x<13\%$) for hole doping. Thus some ingredient in addition to the t-J model may be needed to explain the experimental observation of superconductivity at $x=0.35$ in electron-doped $Na_xCoO_2\cdot yH_2O$. Exploration of the $Na_{1-x}TiO_2$ system may be more promising. We also note that $Na_{0.7}CoO_2$ is a metal which exhibits unusual behavior such as linear T resistivity and large magnetic-field-dependent thermal power.[21] This is also inconsistent with the mean-field prediction of Fermi liquid in the overdoped region, suggesting that some additional physics may be at work. In any event, the observation opens up the possibility of changing the doping concentration in a controlled way by intercalation and much new physics surely remains to be discovered.

After the completion of this work we have seen a paper by Kumar and Shastry[22] reaching similar conclusions. However, we do not agree with their identification of the sign of t.

We thank Fangcheng Chou, Joel Moore, T.K. Ng, and N.P. Ong for helpful discussions. Q.H.W. was supported by NSFC Grant Nos. 10204011, 10325416, 10021001, and by the Ministry of Science and Technology of China (NKBRSF Grant No. G1999064602). He also thanks Z. D. Wang for hospitality in the University of Hong Kong. D.H.L. was supported by DOE Grant No. DE-AC03-76SF00098. P.A.L. was supported by NSF Grant No. DMR-0201069. He also acknowledges the Miller Institute at Berkeley for support.

[1] J.G. Bednorz and K.A. Müller, Z. Phys. B: Condens. Matter **64**, 189 (1986).
[2] P.W. Anderson, Science **235**, 1196 (1987).
[3] K. Takada, H. Sakurai, E. Takayama-Muromachi, F. Izumi, R.A. Dilanian, and T. Sasaki, Nature (London) **422**, 53 (2003).
[4] G. Baskaran, Phys. Rev. Lett. **91**, 097003 (2003).
[5] S.Yu. Ezhov, V.I. Anisimov, H.F. Pen, D.I. Khomskii, and G.A. Sawatzky, Europhys. Lett. **44**, 491 (1998).
[6] D.J. Singh, Phys. Rev. B **61**, 13397 (2000).
[7] T. Valla, P.D. Johnson, Z. Yusof, B. Wells, Q. Li, S.M. Loureiro, R.J. Cava, M. Mikami, Y. Mori, M. Yoshimura, and T. Sasaki, Nature (London) **417**, 627 (2002).
[8] A. Seidel, C.A. Marianetti, F.C. Chou, G. Ceder, and P.A. Lee, Phys. Rev. B **67**, 020405 (2003).
[9] S.J. Clarke, A.C. Duggan, A.J. Fowkes, A. Harrison, R.M. Ibberson, and M.J. Rosseinsky, Chem. Commun. (Cambridge) **1196**, 409 (1996).
[10] J. Brinckmann and P.A. Lee, Phys. Rev. B **65**, 014502 (2001).
[11] D.A. Huse and V. Elser, Phys. Rev. Lett. **60**, 2531 (1988).
[12] Jung Hoon Han, Qiang-Hua Wang, and Dung-Hai Lee, Int. J. Mod. Phys. **15**, 1117 (2001).
[13] V. Kalmeyer and R.B. Laughlin, Phys. Rev. Lett. **59**, 2095 (1987).
[14] T.K. Lee and S. Feng, Phys. Rev. B **41**, 11110 (1990).
[15] For BEC calculation, an artificial tiny dispersion in the z direction is needed. See, e.g., G. Kotliar and J. Liu, Phys. Rev. B **38**, 5142 (1988).
[16] P.A. Lee and X.-G. Wen, Phys. Rev. Lett. **78**, 4111 (1997).
[17] J. Corson, R. Mallozzi, J. Orenstein, J.N. Eckstein, and I. Bozovic, Nature (London) **398**, 221 (1999).
[18] B.I. Halperin, J. March-Russell, and F. Wilczek, Phys. Rev. B **40**, 8726 (1989).
[19] B. Braunecker, P.A. Lee, and Ziqiang Wang (unpublished).
[20] T. Senthil, J.B. Marston, and M.P.A. Fisher, Phys. Rev. B **60**, 4245 (1999).
[21] I. Terasaki, Y. Sasago, and K. Uchinokura, Phys. Rev. B **56**, 12685 (1997); Y.Y. Wang, N.S. Rogado, R.J. Cava, and N.P. Ong, Nature (London) **423**, 425 (2003).
[22] B. Kumar and B.S. Shastry, Phys. Rev. B **68**, 104508 (2003).